Deterministic spatiotemporal control of optical fields in nanoantennas and plasmonic circuits

J. S. Huang,[1,*] D. V. Voronine,[2] P. Tuchscherer,[2] T. Brixner,[2] and B. Hecht[1,†]

[1]*Nano-Optics and Biophotonics Group, Experimentelle Physik 5 and Wilhelm-Conrad-Röntgen Center for Complex Material Systems (RCCM), Physikalisches Institut, Universität Würzburg, Am Hubland, 97074 Würzburg, Germany*

[2]*Institut für Physikalische Chemie, Universität Würzburg, Am Hubland, 97074 Würzburg, Germany*

(Received 13 January 2009; revised manuscript received 7 May 2009; published 29 May 2009)

We show that laser pulse shaping techniques can be applied to tailor the ultrafast temporal response of localized and propagating optical near fields in resonant optical antennas (ROAs) and plasmonic transmission lines, respectively. Using finite-difference time-domain simulations followed by Fourier transformation, we obtain the impulse response of a nanostructure in the frequency domain, which allows obtaining its temporal response to any arbitrary pulse shape. To illustrate the potential of the method we demonstrate deterministic optimal temporal pulse compression in ROAs with reduced symmetry, in a plasmonic two-wire transmission line, and in a prototype plasmonic circuit combining propagation effects and local resonances. The method described here will be of importance for the coherent control of field propagation in nanophotonic structures and light-induced processes in nanoscopic volumes.

DOI: 10.1103/PhysRevB.79.195441 PACS number(s): 78.67.−n, 73.21.−b, 84.40.Az, 84.40.Ba

Spatiotemporal control of strongly enhanced optical fields with nanometer and femtosecond resolutions is a key challenge in nano-optics.[1] In terms of spatial confinement of light, much effort has recently been devoted to study the optical resonant behavior of plasmonic nanostructures,[2–6] among which resonant optical antennas (ROAs) excel in intensity enhancement (~1000 times) (Refs. 7 and 8) and spatial confinement (10 nm characteristic length). Well-designed ROAs govern the radiation of emitters in their vicinity[9–11] and provide the basis for enhanced single-photon sources,[10,12] antenna-enhanced local spectroscopy,[13–15] and a broad range of applications.[16–19] Structures that are able to guide optical fields with deep subwavelength mode extension have also been explored extensively[20–22] in view of possible plasmonic circuitry.[23–25] Coherent control of near fields by phase, amplitude, and polarization pulse shaping in plasmonic nanostructures has recently been theoretically proposed[26–31] and experimentally realized.[32,33] Applying the concepts of coherent spatiotemporal control for tailoring the near-field response of plasmonic nanostructures entails understanding of how the resonant character of nanostructures and propagation effects determine the temporal response in a chosen point in space.

Here we propose a way of using the finite-difference time-domain (FDTD) method to simulate the near-field response of a nanostructure to arbitrarily shaped laser pulses. We suggest to perform a time-domain calculation only once, followed by a Fourier transformation to the spectral domain from which the impulse response of the structure is calculated. Using this impulse response, the near-field responses to any desired pulse shape can be obtained by a multiplication in the spectral domain. Since our approach is based on the linear Maxwell's equations, here solved by means of the FDTD algorithm, such calculations are generally valid regardless of the nanostructure shape. Compared to previous studies[26] we avoid repeating costly simulations for each new pulse shape. This method, therefore, provides a powerful tool to explore the effects of pulse shaping in nano-optics. In general, the near-field optical response of any complex structure can be described in terms of combinations of two fundamental coupling effects, i.e., (i) coupling of localized resonances and (ii) continuous propagation of guided modes with dispersion. We, therefore, demonstrate the power of this approach by considering two structures, a displaced-gap linear dipole antenna and a plasmonic transmission line, which represent the two fundamental coupling effects, as well as an optical circuit combining both effects.

First, we show that by applying pulses with an opposite phase with respect to the impulse response, optimal temporal compression is achieved in asymmetric ROAs. We then demonstrate that laser pulse shaping can also be used to compensate and control pulse broadening due to dispersion in a nanosize plasmonic two-wire transmission line excited via a ROA.[34] We, therefore, extend the classical experiments of adaptive pulse compression[35,36] and the concept of energy localization in random nanostructures[27,31] to the deterministic spatiotemporal control of nano-optical fields. Although in the present paper we concentrate on the possibility to achieve temporal compression, our technique is naturally not limited to time domain but can also be used to deterministically tailor arbitrary temporal and spectral shapes of ultrafast near fields, which is a prerequisite for coherent control at the nanometer scale as well as for the operation of nanophotonic integrated circuits and related applications.

Efficient ROAs can be realized using noble-metal nanorods. The plasmon resonances of individual rods are determined by their dimensions and dielectric function[2] or equivalently by length-dependent Fabry-Pérot resonances of a plasmon wave[4] propagating with an effective wavelength[5] along the rod and being reflected at its ends. While a single rod may be considered a monopole antenna,[11] dipole antennas are formed by aligning two nanorods end to end, thus creating a very small feed gap where optical fields are concentrated and enhanced.[8] An *x*-polarized 10 fs laser pulse centered at 711 nm is used as a default source in the FDTD simulations[37] (see Fig. 1). The source is a focused Gaussian beam (numerical aperture 1.0) which is injected from within the silica half space with perpendicular incidence on the silica-air interface. Since only *x*-polarized excitation is considered, its electric field may be expressed as a scalar,

 ©2009 The American Physical Society

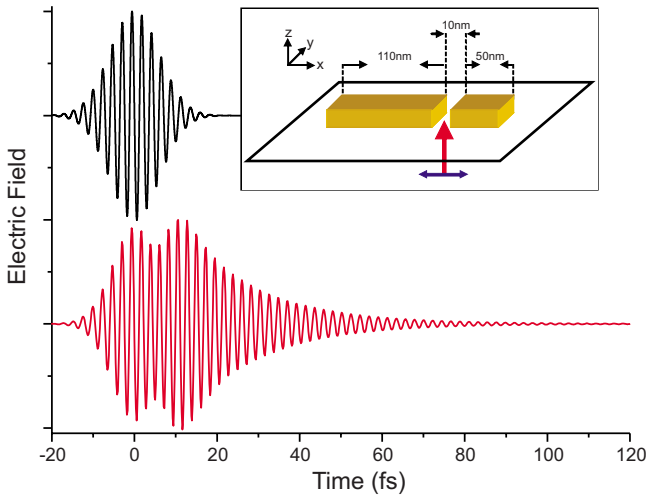

FIG. 1. (Color online) Time-dependent electric fields of the default excitation source (black, top) and the corresponding near-field response (red, bottom) at the feed gap center of a dipole antenna with a displaced gap. Antenna dimensions are $20\times20\times170$ nm^3 including a 10 nm gap, which is shifted 30 nm away from the antenna center. The displaced gap results in arm lengths of 110 and 50 nm as sketched in the inset.

$$S(t) = S_0 e^{-(1/2)[(t-t_0)/\Delta t]^2} \sin[\omega(t-t_0)], \tag{1}$$

where S_0 is the peak amplitude of the source electric field, t_0 is the time offset of the pulse, Δt is the pulse duration, and ω is the carrier angular frequency. The default source has a flat spectral phase (no chirp). The nanostructures to be investigated are made of gold on silica substrates in air. We use the multicoefficient model[37] to fit the dielectric functions of gold and silica.[38,39] Structures are discretized using mesh steps in x, y, and z directions of 1 nm to obtain reliable results with reasonable simulation time. All the structures have faces and edges parallel to the rectangular mesh grid. We, therefore, exclude the influence of spurious resonances due to staircasing effects. All boundaries of the total simulation cube contain 12 perfectly matched layers and are set to be more than 400 nm away from the metal structure surfaces to avoid absorption of near fields.

We first study the temporal response of a dipole antenna with a displaced gap, i.e., an antenna consisting of two gold nanorods with the same cross section (20×20 nm^2) but different length (110 and 50 nm) separated by a feed gap of 10 nm as depicted in the inset of Fig. 1. FDTD simulations provide the time-dependent electric fields $\mathbf{E}(t)$ in the vicinity of the structure, e.g., in the feed gap (bottom red trace in Fig. 1). Both, the source field $S(t)$ (top black trace in Fig. 1) and the corresponding response of the structure are Fourier transformed to yield the respective quantities $S(\omega)$ and $\mathbf{E}(\omega)$ in the frequency domain. The so-called impulse response function for any desired point $\mathbf{r}$ in the vicinity of the structure is now obtained by normalizing the response of the structure with the source spectrum

$$\mathbf{E}_{\text{impulse}}(\omega,\mathbf{r}) = \frac{\mathbf{E}(\omega,\mathbf{r})}{S(\omega)}. \tag{2}$$

Note that the electric fields are vectors, therefore, near-field depolarization effects are taken into account. The validity of this equation is independent of the observation position.[40] However, in the present example of a displaced-gap linear dipole antenna, the field component along the antenna (E_x) dominates in the feed gap.[8] Since the frequency dependence due to the finite pulse length of the source has been removed, the impulse spectrum reveals the spectral response of the structure to a δ-function pulse. It, therefore, serves as a Green's function in the frequency domain. The new local response $\mathbf{E}_{\text{new}}(\omega,\mathbf{r})$ to any chosen source pulse shape $S_{\text{shaped}}(\omega)$ can be simply obtained by multiplying the impulse response with the new source in the spectral domain,

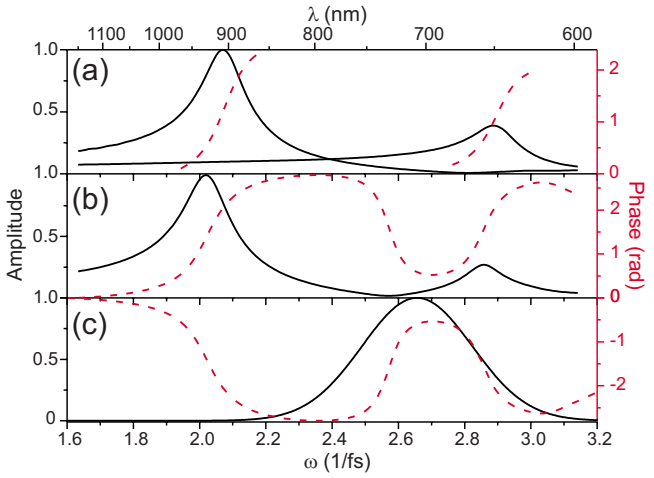

FIG. 2. (Color online) (a) Source-independent impulse spectra (black solid line) and spectral phase (red dashed line) of isolated 50 nm and 110 nm gold nanorods recorded at a point on the long axis of the rod, 5 nm from its end in air. (b) Source-independent impulse spectrum (black solid line) and spectral phase (red dashed line) of the respective displaced-gap antenna consisting of the two rods in (a), recorded at the center of the 10 nm feed gap. The amplitude scale in (b) is about 30 times larger than in (a) due to antenna enhancement. (c) Spectrum (black solid line) and phase (red dashed line) of a new source pulse. The new phase is shaped as the opposite of the displaced-gap antenna spectral phase shown in (b). All amplitudes are normalized to unity.

$$\mathbf{E}_{\text{new}}(\omega,\mathbf{r}) = S_{\text{shaped}}(\omega)\mathbf{E}_{\text{impulse}}(\omega,\mathbf{r}). \tag{3}$$

A higher-order nonlinear spectral phase of the impulse response directly reveals a possible chirp introduced by the nanostructure. In the case considered here, each individual antenna arm exhibits its own longitudinal plasmon resonance with the expected harmonic-oscillator behavior of the phase. The impulse spectrum of a displaced-gap antenna shows two clear resonance peaks due to asymmetry.[41] These two peaks around the angular frequencies 2.02 fs^{-1} (930 nm) and 2.85 fs^{-1} (659 nm) correspond to 110 and 50 nm single gold nanorod resonances, whose impulse spectra and phases are shown in Fig. 2(a). The longer rod resonance is shifted to the red and shows a stronger near-field enhancement due to the fact that the longitudinal plasmonic resonance is redshifted and becomes stronger as the aspect ratio of the rod increases.[2] We observe that for a *single* rod excited by linearly polarized light along the long axis [see Fig. 2(a)] and also for a *symmetric* dipole antenna (data not shown) the

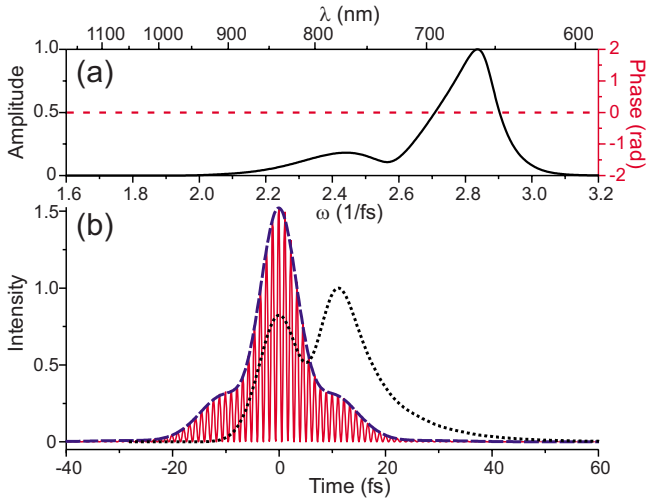

FIG. 3. (Color online) (a) New response spectrum (black solid line) and spectral phase (red dashed line). The amplitude is normalized to unity. (b) Temporal intensity profiles of the original response (black dotted line) and of the new response evaluated directly from Eq. (3) followed by an inverse Fourier transformation (blue dashed line). For comparison, we also plot the square of the real part of the electric field (red solid line) obtained from a full FDTD simulation with the shaped source shown in Fig. 2(c). All intensities are normalized to the maximum intensity of the original response.

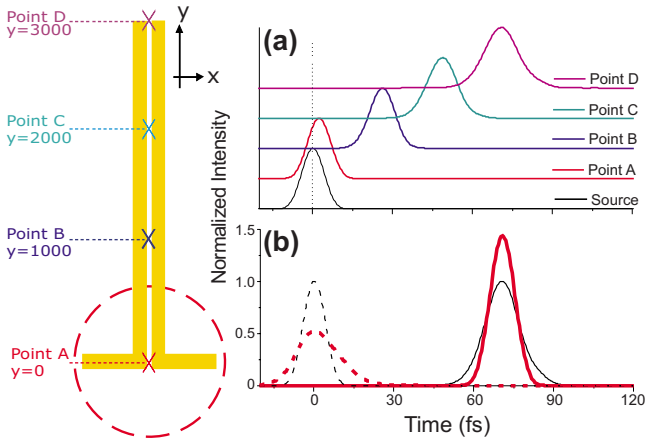

FIG. 4. (Color online) Left panel: sketch of the transmission line and the observation points. Two long gold nanowires with 20×20 nm^2 cross section and 10 nm separation are attached to two arms of a $20\times20\times190$ nm^3 antenna. The red dashed circle denotes the excitation area. Observation: point A is located at the feed gap center, while points B–D are shifted in the $+y$ direction from point A by 1000, 2000, and 3000 nm, respectively. Right panel: (a) normalized temporal intensity profiles recorded at points A (red), B (blue), C (green), and D (pink) obtained with the default source (black); (b) normalized original (black thin line) and new (red thick line) temporal intensity profiles of the source (dashed) and the response (solid) at point D.

spectral phase around the resonance is linear to a good approximation,[42] thus negligible chirp is introduced. This is supported by recent experiments on symmetric bow-tie antenna arrays.[16]

While in view of applications this is an important finding in itself, we also observe that already the presence of a second resonance due to an asymmetric feed gap, not to speak of more complicated structures with more resonances, introduces higher-order spectral phase behavior as illustrated in Fig. 2(b). But since the impulse response of the structure is known, it is possible to deterministically precompensate any pulse broadening by adapting the source pulse shape such that its spectral phase is the opposite of the impulse response spectral phase as illustrated in Fig. 2(c). As a result, the response of the structure to the so-modified source exhibits a flat spectral phase and is optimally compressed in time.[35,36] Most importantly, the structure's response to any chosen source pulse shape can be simply obtained by multiplying the impulse response with the new source in the spectral domain without rerunning expensive FDTD simulations. This feature will be particularly useful for finding optimal pulse shapes when using evolutionary algorithms.

Applying the shaped pulse to the structure, the dispersion is precompensated and a new response with a flat phase is obtained as shown in Fig. 3(a). The new source excites both resonances due to the broad bandwidth of the ultrashort pulse. This results in the main peak at $\omega=2.85$ fs^{-1} and a shoulder around $\omega=2.45$ fs^{-1}. Since the spectral phase is flat, the temporal broadening is removed. As a result, the new response is compressed in time and its temporal width is finally limited by the Q factor of the relevant plasmon resonance provided the excitation pulse is sufficiently short. Figure 3(b) shows the original response along with the temporal intensity profile of the well-compressed new response obtained by Eq. (3) and inverse Fourier transformation. The peak intensity is enhanced by a factor of more than 1.5. For comparison, here we also plot the square of the real part of the electric field obtained from a full FDTD simulation with the shaped source shown in Fig. 2(c). The perfect coincidence between the full FDTD simulation and the much faster evaluation of Eq. (3) demonstrates the validity of our approach. In all other examples we only use Eq. (3). Because both resonances of the structure are excited, the compressed temporal profile in Fig. 3(b) is not a Gaussian but has shoulders. Although we determine the linear response, the peak intensity enhancement as observed in the present example of an asymmetric dipole antenna will be of importance for nonlinear phenomena occurring in the antenna feed gap[8,43] or higher-order harmonic signals sensitive to the local field intensity.[16,42]

Further, we study a two-wire plasmonic transmission line.[34] The equivalent circuit for the transmission line is a chain of interacting resonant circuits each representing an infinitely short section of the transmission line.[44] The effect of these interacting resonant circuits is that excitations of different frequencies propagate at different velocities along the transmission line, therefore, causing dispersion. To demonstrate the ability of manipulating the temporal profile of a signal traveling down the transmission line, we attached a symmetric dipole antenna to it,[34,45] as shown in Fig. 4. A symmetric antenna is used here to efficiently excite the fundamental guided mode without introducing significant chirp itself. Upon illumination of the dipole antenna, the field is first spatially confined and enhanced in the feed gap and then travels as a strongly confined quasi-TE mode between the

two wires of the transmission line. We have recently found that these nanotransmission lines at optical frequencies behave quite similar to those in the rf regime.[34] Concepts of classical electronic circuits, e.g., impedance matching, are well applicable.[34,46] A propagating pulse along such transmission line is expected to be broadened by group-velocity dispersion[47] and phase modulation in analogy to effects also known from optical fibers.[48] As shown in Fig. 4(a), the temporal responses obtained at different positions along the transmission line show broadening which is increasing with the distance traveled. This temporal broadening, along with Ohmic losses, rapidly diminishes the peak intensity of the signal. By applying a phase-shaped pulse to the incoupling antenna using the method outlined above, the signal is recompressed at point D and the field intensity is improved by a factor of 1.5 as shown in Fig. 4(b). In addition to the compression at point D, the new source shows a broader temporal intensity profile and a lower peak intensity with the same pulse energy. Since the local field is highly enhanced in the feed gap and easily exceeds the damage threshold,[7,8,16,49] this broadened excitation pulse may prevent the structure from being damaged by the source. So far, we have shown that our approach can be used to compress both localized and propagating optical near fields. As the complexity of the investigated structures increases so does the number of resonances that determine the response of a structure to an excitation with a short laser pulse, causing a stronger temporal broadening of the near field. As an example of a more general case, we apply our method to a complex structure (sketched in Fig. 5) consisting of a displaced-gap receiving antenna connecting to a finite-length transmission line with two branches terminated by two emitting antennas. This structure represents a prototype photonic circuit in which signals suffer from temporal broadening due to both coupling of localized resonances and dispersion of propagating fields as is the case in any general plasmonic structure. As shown in Figs. 5(a) and 5(b), broadened signals can deterministically be recompressed in time regardless of the structure's complexity.

In conclusion, the FDTD method is useful to simulate the impulse response of plasmonic nanostructures with multiple resonances. Responses to arbitrary source pulse shapes can be obtained, without rerunning expensive FDTD simulations, from a simple multiplication of a new source and the impulse response in the spectral domain followed by an inverse Fourier transformation. The validity of this approach is demonstrated by a comparison to full FDTD simulations. The temporally broadened localized fields of an optical antenna or propagating transmission line modes can be recompressed by deterministic shaping of the source spectral phase thus enhancing the peak intensities in the structure. This method is general and will be of importance for future experiments involving coherent control of field propagation in nanophotonic devices and light-induced processes in nanometer scale volumes. In addition to spatiotemporal compression of local fields, the method presented here allows optimizing the temporal response of real optical antennas and more complex structures which deviate from the ideal shape and, therefore, sets the basis for future subwavelength coherent control applications.

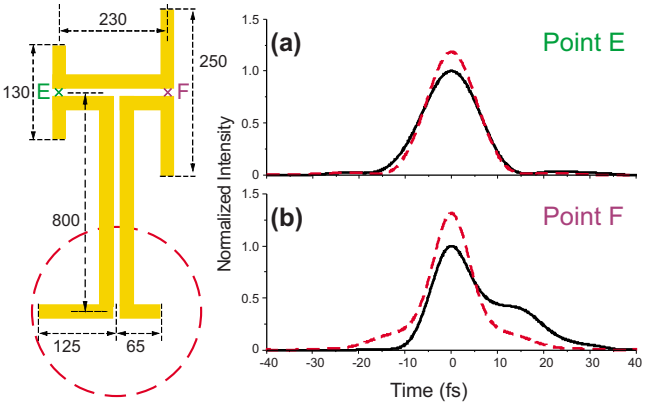

FIG. 5. (Color online) Left panel: sketch of an optical circuit and the observation points. The circuit consists of three antennas and a finite-length plasmonic transmission line with a *T* branching. All wires and antennas have a 20×20 nm^2 quadratic cross section and 10 nm gap. Dimensions are indicated in nanometers. The red-dashed circle denotes the excitation area. Observation: points E and F are located at the feed gap centers of the left and right antennas, respectively. Right panel: normalized original (black solid line) and new (red dashed line) temporal intensity profiles of signals recorded at (a) point E and (b) point F.

B.H. and J.S.H. thank T. Feichtner for helpful discussions and the Wolfermann-Nägeli Foundation for financial support. Funding by the DFG is acknowledged through the Emmy-Noether Program (T.B.) and the SPP 1391 "Ultrafast Nano-Optics."

*jhuang@physik.uni-wuerzburg.de
†hecht@physik.uni-wuerzburg.de

[1] L. Novotny and B. Hecht, *Principles of Nano-Optics* (Cambridge University Press, New York, 2006).
[2] S. Link and M. A. El-Sayed, J. Phys. Chem. B **103**, 8410 (1999).
[3] E. Prodan, C. Radloff, N. J. Halas, and P. Nordlander, Science **302**, 419 (2003).
[4] H. Ditlbacher, A. Hohenau, D. Wagner, U. Kreibig, M. Rogers, F. Hofer, F. R. Aussenegg, and J. R. Krenn, Phys. Rev. Lett. **95**, 257403 (2005).
[5] L. Novotny, Phys. Rev. Lett. **98**, 266802 (2007).
[6] F. Hao, Y. Sonnefraud, P. Van Dorpe, S. A. Maier, N. J. Halas, and P. Nordlander, Nano Lett. **8**, 3983 (2008).
[7] P. J. Schuck, D. P. Fromm, A. Sundaramurthy, G. S. Kino, and W. E. Moerner, Phys. Rev. Lett. **94**, 017402 (2005).
[8] P. Mühlschlegel, E.-J. Eisler, O. J. F. Martin, B. Hecht, and D. W. Pohl, Science **308**, 1607 (2005).
[9] R. J. Moerland, T. H. Taminiau, L. Novotny, N. F. van Hulst, and L. Kuipers, Nano Lett. **8**, 606 (2008).
[10] J. N. Farahani, D. W. Pohl, H.-J. Eisler, and B. Hecht, Phys. Rev.

Lett. **95**, 017402 (2005).
[11] T. H. Taminiau, R. J. Moerland, F. B. Segerink, L. Kuipers, and N. F. van Hulst, Nano Lett. **7**, 28 (2007).
[12] O. L. Muskens, V. Giannini, J. A. Sánchez-Gil, and J. Gómez Rivas, Nano Lett. **7**, 2871 (2007).
[13] D. P. Fromm, A. Sundaramurthy, A. Kinkhabwala, P. J. Schuck, G. S. Kino, and W. E. Moerner, J. Chem. Phys. **124**, 061101 (2006).
[14] N. Anderson, P. Anger, A. Hartschuh, and L. Novotny, Nano Lett. **6**, 744 (2006).
[15] C. Höppener and L. Novotny, Nano Lett. **8**, 642 (2008).
[16] S. Kim, J. Jin, Y.-J. Kim, I.-Y. Park, Y. Kim, and S. W. Kim, Nature (London) **453**, 757 (2008).
[17] A. M. Gobin, M. H. Lee, N. J. Halas, W. D. James, R. A. Drezek, and J. L. West, Nano Lett. **7**, 1929 (2007).
[18] A. Drezet, C. Genet, and T. W. Ebbesen, Phys. Rev. Lett. **101**, 043902 (2008).
[19] D. E. Chang, A. S. Sorensen, E. A. Demler, and M. D. Lukin, Nat. Phys. **3**, 807 (2007).
[20] J. Takahara, S. Yamagishi, H. Taki, A. Morimoto, and T. Kobayashi, Opt. Lett. **22**, 475 (1997).
[21] S. I. Bozhevolnyi, J. Erland, K. Leosson, P. M. W. Skovgaard, and J. M. Hvam, Phys. Rev. Lett. **86**, 3008 (2001).
[22] S. I. Bozhevolnyi, V. S. Volkov, E. Devaux, J.-Y. Laluet, and T. W. Ebbesen, Nature (London) **440**, 508 (2006).
[23] W. L. Barnes, A. Dereux, and T. W. Ebbesen, Nature (London) **424**, 824 (2003).
[24] E. Ozbay, Science **311**, 189 (2006).
[25] S. A. Maier, IEEE J. Sel. Top. Quantum Electron. **12**, 1214 (2006).
[26] M. Sukharev and T. Seideman, J. Phys. B **40**, S283 (2007).
[27] M. I. Stockman, S. V. Faleev, and D. J. Bergman, Phys. Rev. Lett. **88**, 067402 (2002).
[28] T.-W. Lee and S. K. Gray, Phys. Rev. B **71**, 035423 (2005).
[29] T. Brixner, F. J. García de Abajo, J. Schneider, and W. Pfeiffer, Phys. Rev. Lett. **95**, 093901 (2005).
[30] T. Brixner, F. J. García de Abajo, J. Schneider, C. Spindler, and W. Pfeiffer, Phys. Rev. B **73**, 125437 (2006).
[31] X. Li and M. I. Stockman, Phys. Rev. B **77**, 195109 (2008).
[32] M. Aeschlimann, M. Bauer, D. Bayer, T. Brixner, F. J. García de Abajo, W. Pfeiffer, M. Rohmer, C. Spindler, and F. Steeb, Nature (London) **446**, 301 (2007).
[33] M. Aeschlimann *et al.*, *Ultrafast Phenomena XVI* (Springer, Berlin, to be published).
[34] J. S. Huang, T. Feichtner, P. Biagioni, and B. Hecht, Nano Lett. **9**, 1897 (2009).
[35] T. Baumert, T. Brixner, V. Seyfried, M. Strehle, and G. Gerber, Appl. Phys. B: Lasers Opt. **65**, 779 (1997).
[36] D. Yelin, D. Meshulach, and Y. Silberberg, Opt. Lett. **22**, 1793 (1997).
[37] FDTD Solutions, Lumerical Solutions, Inc., Vancouver, Canada.
[38] P. B. Johnson and R. W. Christy, Phys. Rev. B **6**, 4370 (1972).
[39] *Handbook of Optical Constants of Solids*, edited by E. D. Palik (Academic, New York, 1985).
[40] See EPAPS Document No. E-PRBMDO-79-118919 for a simple example with a position of observation in the far field. For more information on EPAPS, see http://www.aip.org/pubservs/epaps.html
[41] J. Merlein, M. Kahl, A. Zuschlag, A. Sell, A. Halm, J. Boneberg, P. Leiderer, A. Leitenstorfer, and R. Bratschitsch, Nat. Photonics **2**, 230 (2008).
[42] B. Lamprecht, J. R. Krenn, A. Leitner, and F. R. Aussenegg, Phys. Rev. Lett. **83**, 4421 (1999).
[43] T.-D. Onuta, M. Waegele, C. C. DuFort, W. L. Schaich, and B. Dragnea, Nano Lett. **7**, 557 (2007).
[44] D. K. Cheng, *Field and Wave Electromagnetics*, 2nd ed. (Addison-Wesley, New York, 1983).
[45] D. W. Pohl, in *Near-Field Optics: Principles and Applications*, edited by M. Ohtsu and X. Zhu (World Scientific, Singapore, 2000), pp. 22–23.
[46] A. Alù and N. Engheta, Phys. Rev. Lett. **101**, 043901 (2008).
[47] J. A. Dionne, L. A. Sweatlock, H. A. Atwater, and A. Polman, Phys. Rev. B **72**, 075405 (2005).
[48] B. Nikolaus and D. Grischkowsky, Appl. Phys. Lett. **42**, 1 (1983).
[49] J. Güdde, J. Hohlfeld, J. G. Müller, and E. Matthias, Appl. Surf. Sci. **127-129**, 40 (1998).